

# Carrier Multiplication in Graphene

Torben Winzer, Andreas Knorr, and Ermin Malic\*

*Institut für Theoretische Physik, Technische Universität Berlin, 10623 Berlin, Germany*

E-mail: ermin.malic@tu-berlin.de

## Abstract

Graphene as a zero-bandgap semiconductor is an ideal model structure to study the carrier relaxation channels, which are inefficient in conventional semiconductors. In particular, it is of fundamental interest to address the question whether Auger-type processes significantly influence the carrier dynamics in graphene. These scattering channels bridge the valence and conduction band allowing carrier multiplication - a process that generates multiple charge carriers from the absorption of a single photon. This has been suggested in literature for improving the efficiency of solar cells. Here we show, based on microscopic calculations within the density matrix formalism, that Auger processes do play an unusually strong role for the relaxation dynamics of photo-excited charge carriers in graphene. We predict that a considerable carrier multiplication takes place, suggesting graphene as a new material for high-efficiency solar cells and for high-sensitivity photodetectors.

Graphene is a strictly two-dimensional zero-bandgap semiconductor with a linear energy dispersion. It has exceptional optical and electronic properties, which have sparked interest in both fundamental research and industry.<sup>1-3</sup> The key for designing and engineering novel graphene-based optoelectronic devices is a microscopic understanding of the ultrafast relaxation dynamics of non-equilibrium carriers. To give an example, short relaxation times are crucial for realization

---

\*To whom correspondence should be addressed

high-performance graphene-based saturable absorbers.<sup>4</sup> A further challenging feature of graphene relaxation dynamics is the expected high efficiency of Auger relaxation, which can be exploited to obtain carrier multiplication - a process that has been intensively discussed for improving the efficiency of solar energy conversion.<sup>5-8</sup> Here, multiple charge carriers are generated from the absorption of a single photon. We distinguish two types of Auger processes: Auger recombination (AR) and impact ionization (II), cp. Figure 1. AR is a process, where an electron is scattered from the conduction into the valence band, while at the same time, the energy is transferred to another electron, which is excited to an energetically higher state within the conduction band (Figure 1a). II is the opposite process (inverse Auger recombination): An electron relaxes to an energetically lower state inducing the excitation of a valence band electron into the conduction band (Figure 1b). The result of II is an increase of the carrier density (carrier multiplication). Both processes also occur for holes in an analogous way. In conventional semiconductor structures, these relaxation channels are suppressed by restrictions imposed by energy and momentum conservation, which are difficult to fulfill at the same time due to the bandgap and the energy dispersion. In contrast, graphene is expected to show a very efficient scattering via Auger processes. Here, it is of crucial importance to address the question whether impact ionization is efficient enough to give rise

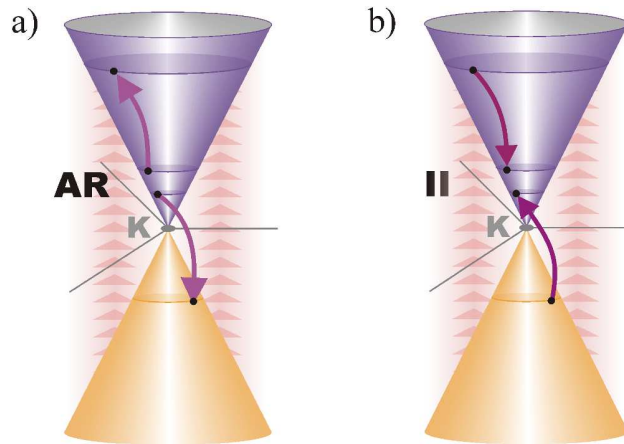


Figure 1: Linear energy dispersion of graphene around the  $K$  point. After an optical excitation (depicted by red arrows), the hot carriers relax toward equilibrium via Coulomb-induced scattering processes. The figure illustrates the two Auger-type relaxation channels: a) Auger recombination (AR) and b) inverse Auger recombination or impact ionization (II).

to a significant carrier multiplication despite the competing processes of Auger recombination, phonon-induced scattering, and intra-band relaxation.

Only few experimental studies on ultrafast relaxation dynamics in graphene have been reported.<sup>9–11</sup> Common to all investigations is the observation of two distinct time scales in differential transmission spectra: A fast initial decay of the pump-induced transmission on a timescale of some tens of femtoseconds and a slower relaxation process in the range of some hundred femtoseconds. The fast decay is ascribed to Coulomb-induced carrier scattering, while the slower process is associated with carrier cooling due to electron-phonon scattering. The experimental data has not yet been complemented by theoretical studies treating all relaxation channels on a consistent microscopic footing. In particular, to best of our knowledge there have been no investigations on the Coulomb-induced fast decay component so far. Previously published reports on the time-resolved relaxation dynamics in graphene focus on the relaxation channels via optical or acoustic phonons accounting for the energy dissipation of photo-excited electrons.<sup>12–14</sup> Others investigated carrier generation and recombination rates based on a static theory.<sup>15</sup> Our microscopic approach, presented in this work, allows a time-resolved study of Auger processes leading to new insights on their efficiency as a function of time starting from the initial non-equilibrium situation up to the achievement of an equilibrium.

In this article, we present a microscopic study of the Coulomb- and phonon-induced relaxation of photo-excited carriers in graphene. Our approach is based on the density matrix formalism describing the coupled population and coherence dynamics including Pauli blocking terms. The starting point for our investigations is the Hamilton operator  $H$  including the non-interacting contribution of carriers and phonons, the electron-light coupling, the Coulomb interaction, and the electron-phonon interaction:  $H = H_0 + H_{\text{carrier-light}} + H_{\text{Coulomb}} + H_{\text{el-ph}}$ . With the above Hamilton operator, we can obtain the temporal evolution of the density matrix elements via Heisenberg equa-

tion<sup>16–19</sup> yielding microscopic many-particle graphene Bloch equations:

$$\dot{f}_{\mathbf{k}}^{\lambda}(t) = 2\text{Im}(\Omega^* p_{\mathbf{k}}) + \Gamma_{\mathbf{k},\lambda}^{\text{in}} (1 - f_{\mathbf{k}}^{\lambda}) - \Gamma_{\mathbf{k},\lambda}^{\text{out}} f_{\mathbf{k}}^{\lambda}, \quad (1)$$

$$\dot{p}_{\mathbf{k}}(t) = -i\Delta\omega_{\mathbf{k}} p_{\mathbf{k}} - i\Omega (f_{\mathbf{k}}^c - f_{\mathbf{k}}^v) - \gamma_{\mathbf{k}} p_{\mathbf{k}} + \sum_{\mathbf{k}'} \gamma_{\mathbf{k}'} p_{\mathbf{k}'}, \quad (2)$$

with the carrier population  $f_{\mathbf{k}}^{\lambda}$  in the conduction ( $\lambda = c$ ) and the valence ( $\lambda = v$ ) band.<sup>17</sup> The microscopic polarization  $p_{\mathbf{k}}$  is a measure for the transition probability. Different terms in the the graphene Bloch equations (color-coded) stem from different Hamilton operator contributions:

(i) The free carrier part  $H_0$  contains the energy dispersion, which is linear around the  $K$  and  $K'$  points,  $\hbar\omega_{\lambda\mathbf{k}} = \pm\hbar v_F |\mathbf{k}|$ , with the electron velocity  $v_F = 10^6 \text{ ms}^{-1}$  and  $\mathbf{k}$  as the wave vector, see Figure 1. It leads to the first term in Eq.(2) with the energy difference between the conduction ( $\lambda = c$ ) and the valence band ( $\lambda = v$ )  $\hbar\Delta\omega_{\mathbf{k}} = \hbar(\omega_{c\mathbf{k}} - \omega_{v\mathbf{k}})$ .

(ii) The carrier-light interaction  $H_{\text{carrier-light}}$  leads to the Rabi frequency  $\Omega(t)$ , which is determined by the the vector potential and the optical matrix element.<sup>20</sup> The excitation field, which optically transfers electrons from the valence band to the conduction band, is described by a Gaussian pulse with the width  $\sigma = 10 \text{ fs}$  and the excitation energy  $\hbar\omega_L = 1.5 \text{ eV}$  (chosen in agreement with a recent experimental realization).<sup>11</sup>

(iii) The Coulomb interaction  $H_{\text{Coulomb}}$  induces scattering between carriers leading to the relaxation of photo-excited electrons and holes. The investigation of non-equilibrium processes requires a description beyond the Hartree-Fock level. We treat the Coulomb interaction up to the second order Born-Markov approximation<sup>17</sup> yielding the Boltzmann-like scattering contributions in equation (1). The time-dependent Coulomb in- and out-scattering rates  $\Gamma_{\mathbf{k}\lambda}^{\text{in/out}}(t)$  are determined microscopically. They explicitly contain intra- and intervalley as well as intra- and interband scattering processes, which fulfill the momentum and the energy conservation. The strength of our approach is the possibility to access the time-, momentum-, and angle-resolved relaxation dynamics of non-equilibrium carriers. For our investigations, we take all relaxation paths into account focusing in particular on Auger-type processes. Electron-phonon scattering - a competing relaxation channel,

is treated on the same microscopic footing.

With all ingredients at hand, we can resolve the relaxation dynamics of photo-excited carriers in graphene: First, electrons are optically excited from the valence into the conduction band by applying a 10 fs laser pulse with an energy of 1.5 eV resulting in a non-equilibrium distribution. The hot charge carriers relax toward equilibrium via Coulomb and phonon-induced scattering processes. For a strong optical excitation, we observe thermalization of carriers within the first hundred femtoseconds followed by carrier cooling induced by electron-phonon scattering. Our results are in agreement with the two decay components observed in experimental differential transmission spectra.<sup>9,11</sup> Furthermore, our investigations show that the intervalley processes play a minor role for the Coulomb-induced relaxation dynamics in graphene. This can be explained by the large momentum transfer, which is necessary to scatter electrons between the valleys. Since the Coulomb matrix element decreases with the momentum transfer, these processes have a negligible contribution. We have also studied the influence of the momentum angle between two scattering electrons. Similar to electron-phonon coupling, where the scattering is maximal for carriers with parallel momenta,<sup>12</sup> electron-electron scattering also shows a pronounced angle-dependence.

Now we can also answer the question whether Auger-type processes play a significant role for the relaxation dynamics in graphene: Figure 2a shows the temporal evolution of the carrier density after an optical excitation. Neglecting all interactions, we can first model the influence of the exciting pulse (red-shaded area in Figure 2 illustrates its width of 10 fs). It generates electrons in conduction and holes in valence band leading to an increase of the charge carrier density  $n$ , as long as the pulse is present (orange line). The inclusion of Coulomb-induced carrier scattering leads to a significant increase of the carrier density, even after the pulse is switched off (purple line). This process - generation of multiple charge carriers by absorption of a single photon - is called carrier multiplication (CM). It is illustrated by the purple-shaded area in Figure 2a. This can be traced back to the process of impact ionization, where valence band electrons are excited

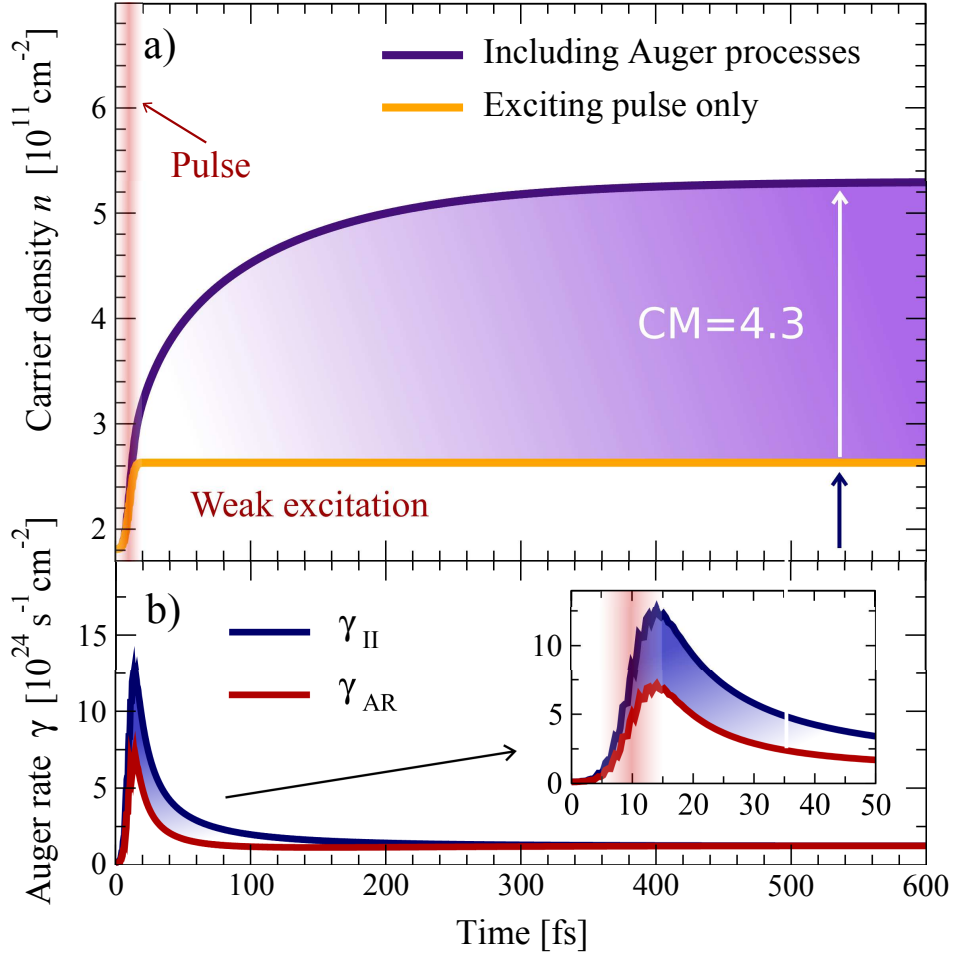


Figure 2: a) Temporal evolution of the charge carrier density  $n$  (electrons in conduction and holes in valence band) for a weak exciting pulse (its width is indicated by the red-shaded area) inducing initial carrier densities in the range of  $10^{11} \text{ cm}^{-2}$ . The figure illustrates the significance of impact ionization leading to carrier multiplication (CM) by a factor of two, i.e. the carrier density induced by the optical excitation (orange line) is doubled during the relaxation process. b) Rates for impact ionization (II) and Auger recombination (AR) as a function of time. The figure illustrates the temporally broad asymmetry between these two Auger processes in favor of II.

into the conduction band, cp. Figure 1b. To prove that our interpretation is correct, we switched off all Auger contributions to the relaxation dynamics. We obtain constant carrier densities after the influence of the pulse. As a conclusion, Auger processes must be responsible for the strong increase of the charge carrier density.

The observed carrier multiplication by a factor of approximately four can be explained by an asymmetry between impact ionization (II) and Auger recombination (AR) resulting in a much higher probability for II. Otherwise, the created carriers would scatter back into the valence band

via AR with the same probability and the carrier multiplication would not occur. The asymmetry can be explained as follows: The squares of the corresponding matrix elements entering the scattering rates  $\Gamma_{k\lambda}^{in/out}(t)$  in Eq.(1) are equal, but the densities of final states for AR and II are quite different, cp. also Ref.<sup>21</sup> To give an example, the probability for an electron to be excited into the conduction band is proportional to  $\Pi \propto f_k^v(1 - f_k^c)$ , while the opposite process is  $\text{AR} \propto f_k^c(1 - f_k^v)$ . In the first femtoseconds after the optical excitation, the probability to find an electron (a hole) in the conduction (valence) band close to the  $K$  point is small, i.e.  $f_k^c \approx 0$  ( $f_k^v \approx 1$ ). As a result,  $\Pi \approx 1$  and  $\text{AR} \approx 0$ . In other words, at the beginning of the relaxation dynamics, the Auger recombination is suppressed by Pauli blocking, since its final states in the valence band are occupied. With increasing relaxation time, an equilibrium between II and AR is reached resulting in a constant carrier density. This interpretation is confirmed by Figure 2b, where the Auger rates  $\gamma_{AR}$  and  $\gamma_{II}$  are shown as a function of time. They are obtained by summing all scattering rates, which contribute to the processes of II and AR, respectively. Figure 2b illustrates the high efficiency of both Auger processes with rates around  $\gamma = 10^{24} \text{ s}^{-1} \text{ cm}^{-2}$ , which is a few orders of magnitudes larger than in conventional GaAs semiconductor quantum wells or InAs/GaAs quantum dots.<sup>22</sup> In the first 300 fs after the excitation, we find a large asymmetry between II and AR with  $\gamma_{II} > \gamma_{AR}$  explaining the observed carrier multiplication in Figure 2a. When the carriers reach equilibrium, the two rates approach the same value  $\gamma_{II} = \gamma_{AR} = 2.5 \cdot 10^{24} \text{ s}^{-1} \text{ cm}^{-2}$ .

The efficiency of carrier multiplication depends on the strength of the optical excitation, i.e. on how many charge carriers are present in the structure and how efficient Pauli blocking and the resulting asymmetry between II and AR is. Figure 3 shows the temporal evolution of the charge carrier density for a strong excitation pulse inducing initial carrier densities in the range of  $10^{13} \text{ cm}^{-2}$ . Here, the Coulomb-induced relaxation dynamics is accelerated, since the number of scattering partners is increased. Auger-type processes as well as intraband carrier-carrier processes become very efficient leading to the thermalization of the electronic system within few tens of femtoseconds, cp. Figure 3b. Both II and AR rates are two orders of magnitude larger than in the case of a weak optical pulse, cp. Figure 2b. However, the asymmetry between II and AR is only given for a

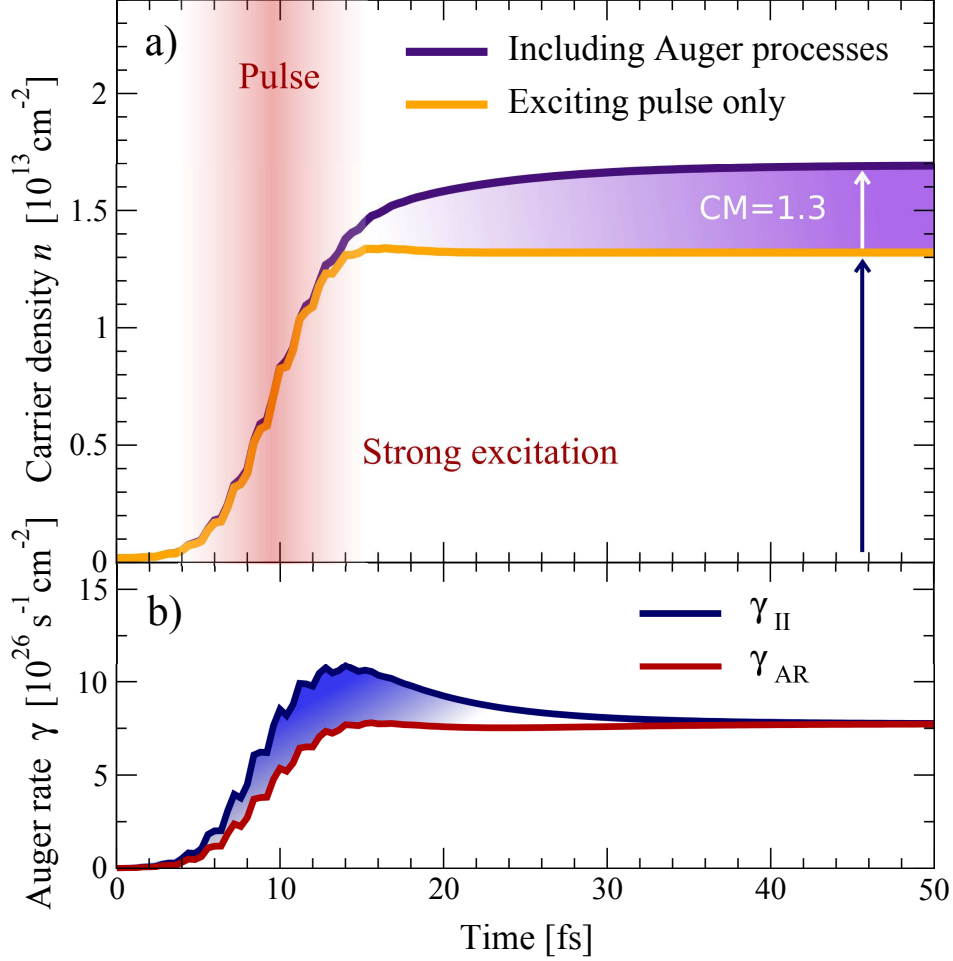


Figure 3: The same as Figure 2, just for the case of a strong excitation pulse, inducing initial carrier densities in the range of  $10^{13} \text{ cm}^{-2}$ . Here, the carrier multiplication (CM) is smaller than in the case of weak excitation, cp. Figure 2a, which can be explained by the temporally narrower asymmetry between the impact ionization and Auger recombination.

narrow time slot, since at high carrier densities an equilibrium is reached very fast. Already after approximately 35 fs, the II and AR rates are equal reaching the value  $\gamma_{II} = \gamma_{AR} = 8 \cdot 10^{26} \text{ s}^{-1} \text{ cm}^{-2}$ . As a result, carriers can be multiplied only during a very short time period leading to a carrier multiplication of 1.3, which is smaller than in the case of weak excitation, cp. Figure 2a. The observed dependence on the exciting pulse intensity, i.e. the carrier density, is in agreement with a first experimental study.<sup>23</sup>

Finally, to study the asymmetry between II and AR, we introduce the Auger scattering time



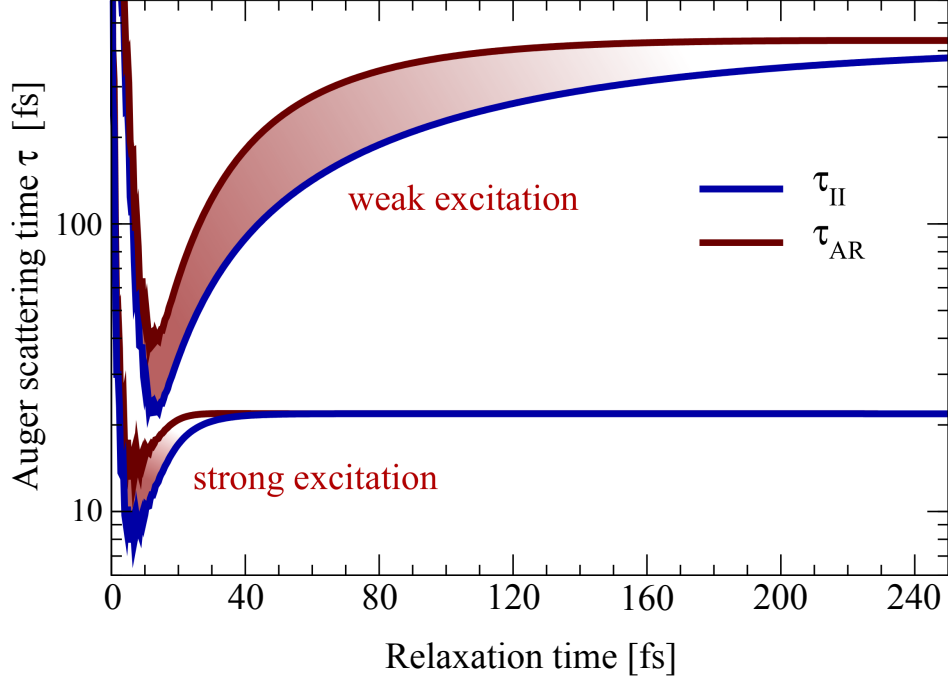


Figure 4: Logarithmic illustration of the asymmetry between the Auger recombination and impact ionization by plotting the corresponding scattering times  $\tau_{II}$  and  $\tau_{AR}$  during the relaxation process for both weak and strong excitation. The region of asymmetry between II and AR (shaded area) is much larger and temporally broader for weak excitation explaining the larger carrier multiplication observed in this case, cp. Figure 2a.

$\tau = n/\gamma$  with the time-dependent carrier density  $n$ , cp. Figure 4. During the first 10 fs, the exciting pulse increases the number of charge carriers resulting in efficient Auger scattering processes, which is reflected by a rapid decrease of the scattering time. In the case of a weak (strong) excitation, the minimal time lies at  $\tau_{II} \approx 20$  fs and  $\tau_{AR} \approx 40$  fs ( $\tau_{II} \approx 8$  fs,  $\tau_{AR} \approx 13$  fs). With increasing relaxation time, the Auger processes become less efficient due to the enhanced Pauli blocking. In equilibrium, the scattering times are  $\tau_{II} \approx 22$  fs and  $\tau_{II} \approx 425$  fs for a strong and a weak exciting pulse, respectively. Figure 4 illustrates that for weak excitation, i.e. small carrier densities, the asymmetry between II and AR is temporally broad offering enough time for a considerable increase of charge carriers. In contrast, for strong excitation II is more efficient only for a small time range directly after the exciting pulse. This results in a smaller value for carrier multiplication.

To understand the efficiency of carrier multiplication, we need to take into account electron-

phonon scattering. This is an important relaxation channel, which is in direct competition with Auger-type processes. Here, the excited electrons are cooled by emission of phonons resulting in a loss of energy necessary for Auger processes. The inclusion of electron-phonon coupling in graphene Bloch equations is straight-forward and yields contributions similar to the electron-electron scattering. For more details, see Ref.<sup>12</sup> As expected, our calculations show that phonons reduce the efficiency of carrier multiplication (not shown). However, it still remains significant enough reflecting the strong Coulomb interaction in graphene and in particular the large and temporally broad asymmetry between II and AR. This finding implies graphene to be a promising candidate for high-sensitivity photodetectors and high-efficiency solar cells. It is beyond the scope of our work to discuss the difficulties one will be confronted with to realize such a device, e.g. the fast extraction of generated carriers before they relax radiatively. We focus on microscopic investigations to give new insights in the temporal dynamics of Auger processes, in particular on the parameter range of an efficient carrier multiplication.

In summary, we have microscopically investigated the charge carrier relaxation and multiplication in graphene. In agreement with recent experiments, we obtain a Coulomb-induced thermalization of the strongly excited system within the first hundred femtoseconds followed by a cooling of carriers via electron-phonon scattering. In particular, we find Auger-type processes to have a significant influence on the relaxation dynamics. We observe a strong asymmetry between impact ionization and Auger recombination leading to a significant multiplication of charge carriers. This process is found to be even more pronounced for very small optical excitations, such as solar radiation. Our calculations reveal that even for small bandgaps of up to 100 meV (modeling graphene nanoribbons), a considerable carrier multiplication still occurs. In conclusion, our fundamental investigations show that Auger-type processes might be of importance for the application of graphene as a new material for high-efficiency solar cells and high-sensitivity photodetectors.

We acknowledge the support from SFB 658 and GRK 1558. Furthermore, we thank U. Woggon (TU Berlin) for discussions on carrier multiplication as well as T. Elsaesser, M. Breusing (MBI

Berlin), and F. Milde (TU Berlin) for discussions on carrier dynamics in graphene.

## References

- (1) Geim, A. K.; Novoselov, K. S. *Nature Materials* **2007**, *6*, 183.
- (2) Neto, A. H. C.; Guinea, F.; Peres, N. M. R.; Novoselov, K. S.; Geim, A. K. *Rev. Mod. Phys.* **2009**, *81*, 109.
- (3) Geim, A. K. *Science* **2009**, *324*, 1530–1534.
- (4) Zhang, H.; Bao, Q. L.; Tang, D. Y.; Zhao, L. M.; Loh, K. *Appl. Phys. Lett.* **2009**, *95*, 141103.
- (5) Nozik, A. J. *Nat. Nanotechnol.* **2009**, *4*, 548–549.
- (6) Nozik, A. J. *Physica E* **2002**, *14*, 115–120.
- (7) McGuire, J. A.; Joo, J.; Pietryga, J. M.; Schaller, R. D.; Klimov, V. I. *Acc. Chem. Res.* **2008**, *41*, 1810–1819.
- (8) Sun, B.; Findikoglu, A. T.; Sykora, M.; Werder, D. J.; Klimov, V. I. *Nano Lett.* **2009**, *9*, 1235–1241.
- (9) Dawlaty, J. M.; Shivaraman, S.; Chandrashekar, M.; Rana, F.; Spencer, M. G. *Phys. Rev. Lett.* **2008**, *101*, 157402.
- (10) Sun, D.; Wu, Z. K.; Divin, C.; Li, X.; Berger, C.; de Heer, W. A.; First, P. N.; Norris, T. B. *Appl. Phys. Lett.* **2008**, *92*, 042116.
- (11) Breusing, M.; Ropers, C.; Elsaesser, T. *Phys. Rev. Lett.* **2009**, *102*, 086809.
- (12) Butscher, S.; Milde, F.; Hirtschulz, M.; Malić, E.; Knorr, A. *Appl. Phys. Lett.* **2007**, *91*, 203103.
- (13) Bistrizter, B.; MacDonald, A. H. *Phys. Rev. Lett.* **2009**, *102*, 206410.

- (14) Tse, W. K.; Sarma, S. D. *Phys. Rev. B* **2009**, *79*, 235406.
- (15) Rana, F. *Phys. Rev. B* **2007**, *76*, 155431.
- (16) Lindberg, M.; Koch, S. W. *Phys. Rev. B* **1988**, *38*, 3342.
- (17) Haug, H.; Koch, S. W. *Quantum Theory of the Optical and Electronic Properties of Semiconductors*; World Scientific, 2004.
- (18) Rossi, F.; Kuhn, T. *Rev. Mod. Phys.* **2002**, *74*, 895.
- (19) Kira, M.; Koch, S. *Progress in Quantum Electronics* **2006**, *30*, 155.
- (20) Malić, E.; Hirtschulz, M.; Milde, F.; Knorr, A.; Reich, S. *Phys. Rev. B* **2006**, *74*, 195431.
- (21) Franceschetti, A.; An, J. M.; Zunger, A. *Nano Lett.* **2006**, *6*, 2191–2195.
- (22) Harrison, P. *Quantum Wells, Wires, and Dots*; Wiley, New York, 2005.
- (23) George, P. A.; Strait, J.; Dawlaty, J.; Shivaraman, S.; Chandrashekar, M.; Rana, F.; Spencer, M. G. *Nano Lett.* **2008**, *8*, .